Calculation Indicates Fractional Quantum Decay is Possible for PbSe Quantum Dots in Inverse-Opal Photonic Crystals

Erwin Schrödinger's famous *gedanken* experiment involving a cat whose fate is determined by whether or not an atom has radioactively decayed was an early illustration of the oddities of quantum mechanics. In his scenario, the probability of the atom not decaying—and thus of the cat surviving—decreases exponentially with time. However, recent advances in the field of photonic crystals have led a number of researchers to investigate the circumstances under which the time-dependence of spontaneous-emission decay in quantum systems can be modified or even eliminated.

P. Kristensen at the Technical University of Denmark, A.F. Koenderink at the FOM Institute for Atomic and Molecular Physics in Amsterdam, and their colleagues have developed a measure of so-called "fractional decay," in which a system never fully decays to its ground state and have theoretically analyzed a realistic physical system in which such an effect should be observed. They report their results in the July issue of *Optics Letters* (DOI: 10.1364/OL.33.001557; p. 1557).

Spontaneous electronic decay in quantum systems is driven by interaction with the vacuum state of the electromagnetic modes to which the system is coupled. For free space and most materials, this coupling is weak, and the structure of these modes is relatively simple, leading to an exponential time dependence of the decay probability. Recently, several groups have noted that there is a regime in which quantum systems interacting coherently with a highly structured electromagnetic mode spectrum, such as that of a photonic crystal, will not fully decay but instead remain in a superposition of ground and excited states. This "fractional decay" has not yet been observed, and previous theoretical analyses have been very general.

The Danish/Dutch group analyzed a specific physical system to determine the parameters under which fractional decay can be expected to occur. In pursuit of this goal, they developed a measure of the extent to which a system undergoes fractional, rather than exponential, decay. Their model system consists of colloidal PbSe quantum dots (QDs) emitting at $\omega_{PbSe} \approx 1.3 \times 10^{15}$ Hz, placed at the *H*–symmetry point in the Wigner–Seitz cell of a closed packed Si inverse-opal photonic crystal whose band edge is slightly detuned from ω_{PbSe}. Beginning with a calculation of the local optical density of states in the photonic crystal, the group analyzed the decay dynamics of the QDs for different amounts of optical loss (absorption) from the Si. While exponential decay dominates for moderate levels of loss, at small but physically realistic loss levels ($\alpha \leq 3 \times 10^{-4}$ cm^{-1}), an appreciable fractional decay effect emerges from the analysis. In the complete absence of loss, the fractional decay effect in the model is strong, and the QD system ultimately settles into a superposition of ground and excited states.

Given these results, it appears reasonable to hope that fractional decay may soon be experimentally observed, marking a significant step forward in ongoing efforts to engineer the behavior of quantum systems.

COLIN MCCORMICK

Modern Technology Unravels Mystery of Ancient Hessian Crucible Manufacturing Process

During the transition from the late Middle Ages to the Renaissance, advances toward higher temperature processes in alchemy, metallurgy, jewelry making, and other areas led to a rise in demand for high-quality ceramic crucibles. After the 12th century, crucible manufacturers from the Hesse region in Germany developed a technique to mass-produce these ceramic vessels with high toughness, refractoriness, and thermal shock resistance. Potters from other European regions unsuccessfully tried to reproduce these high-quality crucibles to such an extent that the quality of the crucibles was dubbed "a mystery."

Centuries later, M. Martinón-Torres of the Institute of Archeology, University College London and his colleagues, along with I.C. Freestone of the School of History and Archeology at Cardiff University decided to apply modern materials-characterization techniques to clarify this mystery. The researchers conducted testing on Hessian and non-Hessian crucibles from 10 different archeological sites.

As reported in the June issue of *The Journal of the American Ceramic Society* (DOI: 10.0000/j.1551-2916.2008.02383.x; p. 2071), the researchers analyzed cross sections of used and unused crucibles by using optical microscopy, scanning electron microscopy, energy dispersive spectroscopy, and x-ray diffraction.

Results revealed a very uniform composition among all specimens analyzed, with 0.4% as the highest standard deviation corresponding to the alumina mean value. Kaolinitic clay with 36.9% alumina composed the ceramic matrix, containing fewer than 5 vol% of impurities. This is evidence of the standardization level reached by this manufacturing process.

Another interesting finding was the presence of abundant quartz sand grains, with a size distribution between 0.25 mm and 1 mm. These grains act as crack arrestors, increasing the fracture toughness resistance of these ceramic vessels. The interfaces of the quartz grains with the ceramic matrix show a level of dissolution, evidence of exposure to a temperature higher than 1200ºC during the firing process. This is consistent with the presence of primary mullite on the ceramic matrix, resulting from the conversion of kaolinite at that temperature level.

Ingenuity and use of local natural resources allowed Hessian crucible makers to determine the correct combination of clay, quartz sand, and firing temperature for the formation of synthetic mullite to produce the earliest examples of such refractory material in Europe, several centuries before this crystal phase was identified.

Fundamental characterization of these ceramic crucibles using electron microscopy and x-ray diffraction techniques provided the researchers with evidence on the resulting phases of each component, and offered enough information to define a range of temperatures and raw material mix conditions and compositions that composed the main recipe for manufacturing these ancient crucibles.

SIARI SOSA

Silsesquioxane Nanoparticle Doping Induces Vertical Alignment in Guest-Host LCDs Without Conventional Alignment Layers

Guest-host liquid crystal displays (GH-LCDs) have desirable features, including high brightness and polarizer-free operation, which have given rise to their popularity in recent years. Typical GH-LCDs require a homeotropic cell with vertical alignment layers to initially align host liquid crystals (LCs) and guest dye molecules perpendicular to the substrate for normally white mode operation.

The industry-adopted method for producing homeotropic LCDs utilizes polyimide alignment layers, which require a high post-curing temperature, precluding the use of this technique for making flexible LCDs using plastic substrates with a low glass transition temperature (Tg). However, W. Teng and colleagues from National Tsing Hua University, Taiwan, along with S. Jeng and colleagues from Industrial Technology Research Institute, Taiwan, have developed a nanoparticle-induced vertical alignment (NIVA) technique to fabricate flexible plastic GH-LCDs without using conventional alignment layers.

The researchers have observed that doping an LC cell with a small amount of polyhedral oligomeric silsequioxane (POSS) nanoparticles induced spontaneous vertical alignment without the need for conventional alignment layers. In the July issue of *Optics Letters* (DOI: 10.1364/OL.33.001663; p. 1663), the researchers described the application of the NIVA technique to fabricate a GH-LCD with normally white characteristics and also made a plastic timepiece. The experimental display medium incorporated 5 wt% aminoethyl-aminopropylisobutyl-POSS nanoparticles along with 5 wt% dichroic dye into negative

Direct Laser Writing and CVD Combined for Fabrication of 3D Photonic Metamaterials

Photonic metamaterials are artificial structures with unusual properties that might lead to quantum levitation, optical cloaking, and lenses for subwavelength imaging. While natural materials at optical frequencies have a magnetic permeability (μ) of unity, metamaterials present researchers with the ability to tune μ to arbitrary values, for example, $\mu < 0$. Usual building blocks of this materials class (typically periodic structures) are split ring resonators (SRRs), which effectively act as "magnetic atoms" with local magnetic dipole moments. Although most photonic metamaterials have been fabricated with two-dimensional techniques—electron-beam lithography and physical evaporation of metal films—and stacking the functional layers, a genuinely three-dimensional (3D) fabrication process is preferable.

Toward this end, M.S. Rill and colleagues at the Institut für Angewandte Physik, Universität Karlsruhe (TH), Germany, and S. Linden and colleagues at the Institut für Nanotechnologie, Forschungszentrum Karlsruhe in der Helmholtz-Gemeinschaft, Germany, have combined direct laser writing (DLW) and silver chemical vapor deposition (CVD) to fabricate a planar test structure composed of elongated SRRs. The researchers found that optical characterization of their structure is in good agreement with theory. Additionally, they fabricated a structure composed of bars, which was metallized uniformly around the structure even in 3D (see Figure 1).

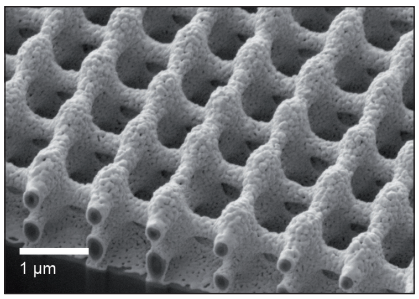

Figure 1. Oblique view of an arrangement of bars fabricated by direct laser writing and silver chemical vapor deposition after it was cut by a focused-ion beam to disclose the interior. The scanning electron micrograph (SEM) shows the potential of the presented technique to fabricate three-dimensional metallic nanostructures. Note that the silver layer covers the bars all around.

As reported in the July issue of *Nature Materials* (DOI 10.1038/nmat2197; p. 543), the researchers made a template from a glass substrate covered with a 2-μm thick polymerized resist film (SU-8). Onto this film, a second SU-8 film was spun, exposing it using DLW, baking, and developing. A thin SiO_2 coating (several dozen nanometers thick), which provides the SU-8 backbone with mechanical stability and chemical protection, was then applied by using atomic layer deposition. CVD of Ag was then performed using the metal–organic precursor (COD)(hfac)Ag(I) at 160°C; about 5 nm of Ag was deposited during a 40-min cycle. The structures resulted from 10 cycles for a total Ag thickness of ~50 nm.

Figure 2 shows a schematic of the structures (with geometrical parameters *a*, *d*, and *w*—the period, height, and width of the arrangement of SRRs, respectively) and an electron micrograph of the actual structure. The Ag coating is uniform, although somewhat granular and, importantly, has no discontinuities, which the researchers demonstrated with good dc conductivity and a reflectance greater than 95% in the wavelength range of 1–4 μm. Normal-incidence transmittance spectra, with incident light polarized vertically to the grooves of the elongated SRRs, showed that different heights (*d*) correspond to different fundamental resonance frequencies.

The researchers said that the effective-medium approximation is well justified, particularly for the structure with $a = 800$ nm and $d = 740$ nm, which shows a value of 4 for λ/a, that is, well separated from the Rayleigh anomalies and the Bragg condition. The researchers then numerically simulated the optical spectra using 3D finite-difference time-domain calculations, which agree well with experiment, and extracted from there the

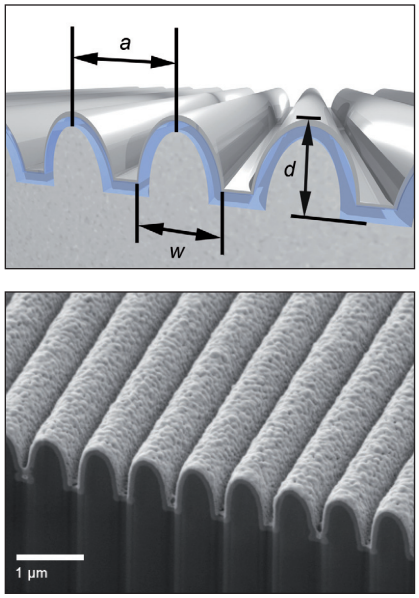

Figure 2. (a) Schematic of a planar lattice of elongated split ring resonators, all metal parts connected; polymer (light grey), silica (blue), and silver (dark grey, reflective). (b) SEM of a metamaterial corresponding to the design schematically shown in Figure 2a. The focused-ion beam cut reveals the SiO_2 layer between the SU-8 template and the silver coating. Reproduced with permission from *Nature Materials* **7** (July) DOI: 10.1038/nmat2197; p. 543. ©2008 Macmillan Publishers Ltd.

effective optical parameters—the complex permittivity, the complex permeability, and the bi-anisotropy parameter, which describes the excitation of magnetic dipoles by the electric component of the field and vice versa. For a fairly broad frequency interval around 100 THz (3 μm wavelength), the real part of μ is negative, showing that the researchers have indeed fabricated a magnetic metamaterial.

The researchers said, "Theory has not yet provided blueprints for 3D metamaterials, but perhaps our approach, which enables rapid prototyping of complex 3D photonic metamaterials, will stimulate theoretical progress."

STEVEN TROHALAKI

https://doi.org/10.1557/mrs2008.170 Published online by Cambridge University Press

dielectric anisotropic LCs, and a test NIVA-GH-LC cell was manufactured using two indium-tin oxide (ITO) substrates separated by 5 µm bead spacers. The test cell exhibited a low threshold voltage of ~2.1 V_{rms} and a high reflectance of ~59% in the voltage-off state.

The researchers reported that optimal vertical alignment depends on the magnitude differences between the POSS-LC and LC-LC interactions. The researchers said that the NIVA phenomenon is due to the adsorption of POSS nanoparticles on the inner surface of the ITO substrates, which lowers the surface tension, thereby inducing homeotropic alignment.

The NIVA technique is advantageous because it can be applied at room temperature and is a relatively simple process for preparing GH-LCDs. The resulting NIVA-GH-LC cells are favorable for low-cost applications, such as price tags and timepieces, which require plastic substrates and low power consumption. The researchers demonstrated this by fabricating a flexible timepiece with 1 wt% dye and 8.5 µm spacers. The next steps are to examine the electro-optical properties and reliability of the plastic NIVA-GH-LC under mechanical bending, said the researchers.

SAMESHA R. BARNES

Terbium Phosphor Exhibits High Spectral Purity in the Green

The color purity of the emission spectrum of terbium-doped crystals excited at wavelengths shorter than 380 nm depends on Tb^{3+} concentration. At low Tb^{3+} concentrations, the emission is dominated by the $^5D_3$-^7F_J (J = 0-6) transitions with several lines in the blue region. With increasing Tb^{3+} concentration, the $^5D_4$-^7F_J transitions become dominant, generating blue, green, yellow, and red lines. However, M. Gusowski and W. Ryba-Romanowski, from the Polish Academy of Sciences in Wroclaw, Poland, reported in the August issue of *Optics Letters* (DOI: 10.1364/OL.33.001786; p. 1786) the development of K_3YF_6:Tb^{3+}—a new phosphor in which, in contrast to other terbium-doped materials reported until now, the emission is independent of the Tb^{3+} concentration and most of the intensity of the green emission was confined in an extremely narrow spectral bandwidth.

The researchers prepared a series of polycrystalline samples $K_3Y_{1-x}Tb_xF_6$ (x = 0.03, 0.1, 0.2, and 1) by heating stoichiometric mixtures of KF_3, YF_3, and TbF_3 at 800ºC in graphite crucibles in Ar atmosphere. They obtained monoclinic crystals with space group $P2_1/n$. Yttrium or terbium ions were sixfold-coordinated by fluorine ions and occupied strongly distorted octahedrons with centrosymmetric C_i local symmetry. The emission spectra were recorded with a fluorometer system consisting of a 150 W xenon lamp coupled to an excitation monochromator and a scanning grating monochromator equipped with a photomultiplier. Excitation at a sample temperature of 8 K by 375 nm light yielded a narrow-band emission at around 545 nm, formed by three line components peaking at 540.77 nm, 541.18 nm, and 541.74 nm, related to transitions from the lowest crystal field component of the $^5D_4$ multiplet to crystal field components of the terminal $^7F_5$ multiplet.

The researchers considered that, although 11 field components were predicted for the $^7F_5$ multiplet of Tb^{3+} in C_i symmetry, only three of them were involved in the emission. The researchers think that pure electric-dipole transitions were forbidden by the centrosymmetric site positions of Tb^{3+} in K_3YF_3, and only the $^5D_4$-$^7F_5$ magnetic-dipole transition remained. When the temperature was increased, an additional line with two distinct maxima grew at longer wavelengths. The long lifetime at room temperature of the $^5D_4$ manifold (14 ms), together with the negligible intensities of other transitions, demonstrate to the researchers that the electron-phonon coupling in this phosphor was low.

The researchers conclude that this phosphor can be efficiently excited in the UV-VUV region through the intense f-d transitions of Tb^{3+} and that it can be of interest for applications requiring high spectral purity in the green region of the electromagnetic spectrum.

JOAN J. CARVAJAL

Railed Microfluidic Channels Enable Precise Microstructure Assembly

Robotic assembly of small parts (<200 µm in size) is difficult because of the precision of the control requirements. Fluidic self-assembly is an alternative approach, which has suffered from low yield because of the probabilistic nature of self-assembly processes. Recently, a simplified manufacturing design was created that has the ability to integrate dissimilar parts into three-dimensional geometries while replicating them in parallel. S.E. Chung, W. Park, and their colleagues at Seoul National University in the School of Electrical Engineering and Computer Science have developed this self-assembly technique using railed microfluidic channels to assemble accurate complex structures.

As described in the July issue of *Nature Materials* (DOI: 10.1038/nmat2208; p. 581), the researchers constructed a microfluidic device out of polydimethylsiloxane (PDMS). Unlike other microfluidic mechanisms, the microchannels of this device have raised structures, called rails, which are grooved on the top surface of the channel. These rails act as a guide for microtrains that contain micro- and nano-size parts that can be photopolymerized *in situ*, transported along the rail-line by fluid flow, and assembled at the end of the rail. The benefit of this technique is that many intricate components of varying materials can be assembled at a high yield.

To show the applicability of this technique, the researchers assembled an array of living cells (to demonstrate the utility of this approach to biomedical applications) and also an array of externally fabricated silicon microchips (to demonstrate the utility of this approach to microelectronic or optoelectronic applications). The living cell matrix, a 3 × 3 hydrogel, was produced by maneuvering two types of living cells (one type transfected by a red fluorescent protein and the other by a green fluorescent protein) into a checkerboard pattern, eliminating multiple lithography steps. The researchers said that this process could be easily adapted to arrays of cells of multiple cell types.

To fabricate the array of microchips, a set of 100 µm × 100 µm silicon chips was propelled through the fluid channel in a polyethylene glycol diacrylate solution. At the end of the rail, a single-step lithography process created an array pattern on the chip with desired spacing. The researchers said that this approach may have commercial applications "for LED [light-emitting diode]-based back-light units or LED lighting packaging where a large number of small LED chips need to be placed in a larger substrate, such as a glass plate or a silicon wafer." From this research, the investigators said that their system may produce nearly zero assembly error in almost any configuration and that railed assembly may be the preferred method of self-assembly of the future.

TARA WASHINGTON

https://doi.org/10.1557/mrs2008.170 Published online by Cambridge University Press